Climate and interannual variability of the atmosphere-biosphere $^{13}CO_2$ flux

M. Scholze

Max-Planck-Institut für Meteorologie, Hamburg, Germany

J. O. Kaplan,[1] W. Knorr, and M. Heimann

Max-Planck-Institut für Biogeochemie, Jena, Germany

[1] We present a bottom-up approach to simulate the terrestrial isotopic carbon variations using the Lund-Potsdam-Jena dynamic global vegetation model (LPJ-DGVM). LPJ is extended to include isotopic fractionation of ^{13}C at the leaf level during assimilation and includes a full isotopic terrestrial carbon cycle. The model thus allows a quantitative analysis of the net biosphere exchange of CO_2 and $^{13}CO_2$ with the atmosphere as a function of changes in climate, atmospheric CO_2, and the isotope ratio of CO_2. LPJ simulates a global mean isotopic fractionation of 17.7‰ at the leaf level with interannual variations of ca. 0.3‰. Interannual variability in the net $^{13}CO_2$ flux between atmosphere and terrestrial biosphere is of the order of 15 PgC‰ yr^{-1}. It is reduced to 4 PgC‰ yr^{-1} if the leaf-level fractionation factor is held constant at the long term mean. Taking climate driven variable fractionation effects into account in double deconvolution studies we estimate that this could imply shifts of up to 0.8 PgC yr^{-1} in the inferred partitioning between terrestrial and oceanic carbon sinks. *INDEX TERMS:* 1615 Global Change: Biogeochemical processes (4805); 0322 Atmospheric Composition and Structure: Constituent sources and sinks; 0315 Biosphere/atmosphere interactions. **Citation:** Scholze, M., J. O. Kaplan, W. Knorr, and M. Heimann, Climate and interannual variability of the atmosphere-biosphere $^{13}CO_2$ flux, *Geophys. Res. Lett.*, *30*(2), 1097, doi:10.1029/2002GL015631, 2003.

1. Introduction

[2] Over the last 50 years anthropogenic emissions of CO_2 added a total of ca. 210 petagrams (10^{15}g) of carbon (PgC) into the atmosphere [*Marland et al.*, 2001]. During the same period the atmospheric CO_2 content increased by 55 ppmv from 310 ppmv CO_2 in 1950 to 365 ppmv CO_2 in 1998 which is equivalent to ca. 115 PgC only [*Prentice*, 2001]. The remaining carbon has been absorbed by the oceans and the land biosphere. Changes in the concentration and $^{13}C/^{12}C$ ratio of atmospheric CO_2 can be used to constrain the global carbon budget and derive location and magnitude of carbon sources and sinks [e.g., *Keeling et al.*, 1989; *Ciais et al.*, 1995; *Heimann and Maier-Reimer*, 1996]. A common method to infer the ocean and land

contributions to these variations is the double-deconvolution of measured records of atmospheric CO_2 and $\delta^{13}C$ ($\delta^{13}C$ is calculated as the deviation with respect to a standard: $\delta^{13}C = \left[\frac{(^{13}C/^{12}C)}{(^{13}C/^{12}C)_{std}} - 1\right] 1000‰$) [*Keeling et al.*, 1989; *Francey et al.*, 1995; *Joos and Bruno*, 1998]. This "top-down" partitioning calculation is sensitive to various quantities, including the assumed isotopic signature of terrestrial carbon, which is usually held constant [e.g., *Keeling et al.*, 1989; *Joos and Bruno*, 1998].

[3] However, the isotopic signature of the terrestrial biosphere is highly variable in space and time. The $\delta^{13}C$ of assimilated CO_2 itself depends strongly on interannual climatic variability and on vegetation composition [*Kaplan et al.*, 2002]. Because of their different anatomy, C_4-plants discriminate against heavy isotopes to a much smaller degree than C_3-plants. The double-deconvolution inversion method requires an a priori representation of the global $^{13}CO_2$ flux field. Our ability to characterize this $^{13}CO_2$ flux field in space and time based on field-scale measurements has not been possible. To date, most inversions have made simplifying assumptions to describe this flux field, e.g., a constant fractionation factor in space in time. Recently, several process-based model representations of the global $^{13}CO_2$ flux field have appeared [*Fung et al.*, 1997; *Kaplan et al.*, 2002]. However, none of these studies have demonstrated how interannual variability in climate affects plant physiology and vegetation dynamics, and through these processes, the $^{13}CO_2$ flux field and its, potentially large, implications for inverse modeling studies.

[4] Here, the dynamic global vegetation model LPJ is used to simulate CO_2 and $^{13}CO_2$ exchange between the atmosphere and biosphere for the last century in a consistent terrestrial carbon cycling framework. A set of experiments are performed to investigate the impact of the processes on the interannual variations in terrestrial carbon isotope discrimination, and to estimate the importance of considering a temporally-variable flux field for inverse modelling studies.

2. Methodology
2.1. The LPJ Dynamic Global Vegetation Model

[5] LPJ [*Sitch et al.*, 2000] combines mechanistic treatment of terrestrial ecosystem structure (vegetation composition, biomass) and function (energy absorption, carbon cycling). Vegetation dynamics are updated annually based on the productivity, disturbance, mortality, and establishment of nine different plant functional types (PFTs). Modelled potential vegetation cover (including C_3-/C_4-plant distribution) depends on competition and climate history.

---

[1]Now at Canadian Centre for Climate Modeling and Analysis, Victoria, Canada.

[6] The enhanced version of LPJ used here fully incorporates ^{13}C as a tracer in the carbon cycle simulated by the model. The carbon isotope module is based on *Kaplan et al.* [2002] which has been validated with measurements at the leaf, canopy, and background atmosphere scales. LPJ, as the successor of the BIOME model used by *Kaplan et al.* [2002], is based on an almost identical formulation of ecosystem structure and function except for the vegetation dynamical elements. The module includes the calculation of isotope fractionation during photosynthesis, the addition of an extra above ground litter pool to represent the age spectrum of decomposing organic matter in a more realistic way, and separate accounting of all internal carbon pools for ^{12}C and ^{13}C.

[7] The isotope discrimination during assimilation is calculated as described by *Lloyd and Farquhar* [1994]. LPJ explicitly simulates the actual inter-cellular-to-atmospheric CO_2 concentration (c_i/c_a) ratio through a coupled photosynthesis and water-balance canopy conductance scheme. Photosynthesis and carbon isotope discrimination are calculated on a daily time step representing daily average values; assimilated CO_2 and $^{13}CO_2$ is allocated to the four different tissue pools (leaves, sap- and heart-wood, roots) on an annual basis. Soil and litter total C and ^{13}C pools are updated monthly. As isotope fractionation processes during respiration are poorly understood, no fractionation is assigned for the decomposition.

2.2. Atmospheric CO_2 and $^{13}CO_2$ Budget

[8] The atmospheric CO_2 budget is given by [e.g., *Tans et al.*, 1993]

$$\frac{d}{dt}N_a = F_f + F_{oc,net} + F_{bnet} = F_s + (F_{ba} - F_{ab}) \quad (1)$$

where F_s is the sum of net ocean and fossil fuel fluxes, F_{ab} is the flux from the atmosphere to the biosphere (here taken as the net primary production, NPP), and F_{ba} is the flux from the biosphere to the atmosphere, i.e., the heterotrophic respiration which here is the sum of the carbon emissions to the atmosphere from the litter and soil pools respectively, and the CO_2 flux due to fire disturbance. Correspondingly the atmospheric $^{13}CO_2$ budget can be formulated as

$$\frac{d}{dt}^{13}N_a = {}^{13}F_f + {}^{13}F_{oc,net} + {}^{13}F_{bnet}$$
$$= {}^{13}F_s + (F_{ba}R_b - F_{ab}\alpha_{ab}R_a) \quad (2)$$

where R_a and R_b are the isotopic ratios of atmospheric and biospheric carbon, respectively, and α_{ab} is the fractionation factor for the atmosphere-biosphere flux. Here, we assume that gross assimilation and autotrophic respiration are in isotopic equilibrium on an interannual time scale [*Ekblad and Högberg*, 2001]. Focusing only on the time dependency of the isotopic ratio R_a and considering only biospheric fluxes it follows with $F_{bnet} = F_{ba} - F_{ab}$ that

$$\left[N_a\frac{d}{dt}R_a\right]_{bios} = F_{bnet}(R_b - R_a) + F_{ab}R_b - F_{ab}\alpha_{ab}R_a \quad (3)$$

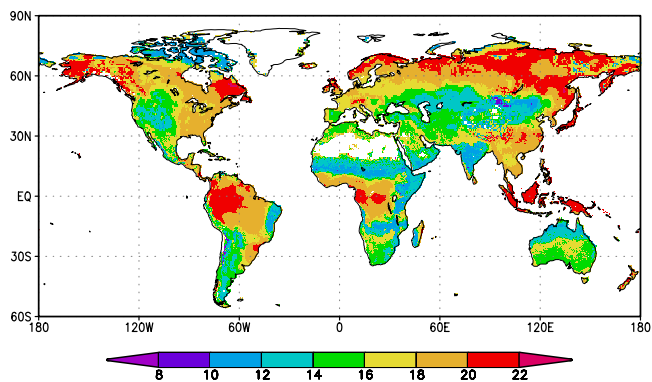[9] Reformulating equation 3 in terms of the δ-Notation (for nomenclature see e.g., *Mook* [1986]) and inserting a

Figure 1. Modelled average (1950–1998) annual values for discrimination against ^{13}C during photosynthesis.

temporal mean (1950–98) fractionation term $\overline{\epsilon_{ab}}$ the temporal change in $\delta^{13}C$ from terrestrial biospheric fluxes can be described with three different terms:

$$\left[N_a\frac{d}{dt}\delta^{13}C_a\right]_{bios} = F_{bnet}(\delta^{13}C_b - \delta^{13}C_a)$$
$$+ F_{ab}(\delta^{13}C_b - (\delta^{13}C_a + \overline{\epsilon_{ab}})) + F_{ab}(\overline{\epsilon_{ab}} - \epsilon_{ab})$$
$$(4)$$

The first term in equation 4 approximates the influence of the variability in the net terrestrial flux on the temporal change in $\delta^{13}C_a$, the second term represents the terrestrial ^{13}C Suess-Effect and the third term $F_{ab}(\overline{\epsilon_{ab}} - \epsilon_{ab}) = \Delta^{13}F_{ab}$ shows the influence of a time-varying fractionation factor on the global $^{13}CO_2$ budget. Global values are obtained by the flux-weighted sum of the quantities at each grid cell, which are then averaged over the globe.

2.3. Set-Up of Model Experiments

[10] Two experiments were performed at $0.5°$ spatial resolution. For both experiments (ISOVAR and ISOFIX) climate forcing data (monthly mean fields of temperature, precipitation, and cloud cover) was taken from the CRU05 1901–1998 monthly climate time-series [*New et al.*, 2000]. In the ISOVAR experiment discrimination was calculated according to the *Lloyd and Farquhar* [1994] scheme as described above, while for the ISOFIX experiment we prescribed a constant discrimination of 18.7‰ for C_3-plants and 3.4‰ for C_4-plants (global mean values from the ISOVAR experiment). For both experiments, we used the time-series of atmospheric CO_2 as described in *McGuire et al.* [2001] and an extended version of the atmospheric $\delta^{13}C$ time-series of *Francey et al.* [1999].

3. Results and Discussion

[11] The modelled leaf discrimination varies from 3‰ to 4‰ for C_4-grasses and 10‰ to 23‰ for C_3-plants. This high variability of up to 13‰ in the leaf discrimination in C_3-PFTs reflects the sensitivity of the discrimination to climate conditions in different regions. The water stress induced by decreasing soil moisture and high water vapour pressure deficit controls the stomatal closure and therefore the c_i/c_a ratio, which is the main variable governing the isotope discrimination. Figure 1 displays the spatial hetero-

Table 1. Mean Discrimination for Two Averaging Periods (1901–1930 and 1950–1998) [‰], the Max. Interannual Variability in Discrimination [‰], and in $\Delta^{13}F_{ab}$ [PgC ‰ yr^{-1}] for Both Experiments

Exp.	Specifications	$\overline{\epsilon_{ab}}$	IAV ϵ_{ab}	IAV $\Delta^{13}F_{ab}$
ISOVAR	var. frac.	17.40	17.67	0.3	15
ISOFIX	const. frac.	17.72	17.75	0.1	4

geneity of the global pattern in the modelled leaf discrimination. The impact of arid climates on discrimination is clearly visible in regions such as central North America and southern South America, Central Asia and in parts also Australia. The influence of C_4-photosynthesis can mainly be seen in the eastern Brazilian grasslands, the African subtropics and the northern region of Australia with discrimination values between 10‰ and 12‰.

[12] The mean globally averaged flux weighted isotopic fractionation $\overline{\epsilon_{ab}}$ over the years 1901–1930 and 1950–1998, the maximum interannual variability of ϵ_{ab}, and of $\Delta^{13}F_{ab}$ are summarized in Table 1 for both experiments. The value from the ISOVAR experiment for the years 1950 to 1998 of 17.7‰ is within the range of values from 14.8‰ to 18.6‰ reported in recent studies [*Keeling et al.*, 1989; *Tans et al.*, 1993; *Lloyd and Farquhar*, 1994; *Fung et al.*, 1997; *Kaplan et al.*, 2002]. Differences arise especially from different amounts of C_4-photosynthesis: while *Lloyd and Farquhar* [1994] (reported value of 14.8‰) prescribe an amount of 25%, in LPJ less then 10% of total carbon is assimilated by C_4-plants, this is partly because of the absence of C_4 land use (pastures and crops). In the ISOFIX experiment, the mean fractionation factor for the period 1950 to 1998 is 17.8‰, almost identical to the ISOVAR experiment.

[13] The interannual variability of ϵ_{ab} in ISOFIX is greatly reduced to 0.1‰ compared to 0.3‰ in ISOVAR as a consequence of the constant fractionation factor (see Figure 2). This remaining variability of ≈0.1‰ is entirely caused by changes from C_3- to C_4-plants and their productivity. The long-term trend in discrimination in the ISOVAR experiment could have two possible explanations: first increasing atmospheric CO_2 content changed the c_i/c_a ratio and the discrimination factor, or second a long-term trend in climate had a direct effect on discrimination. In a third experiment with constant climate but variable CO_2, the discrimination factor did not show any trend over the 98 years. Therefore we assume that the trend in the ISOVAR
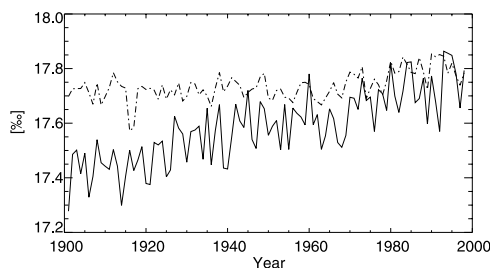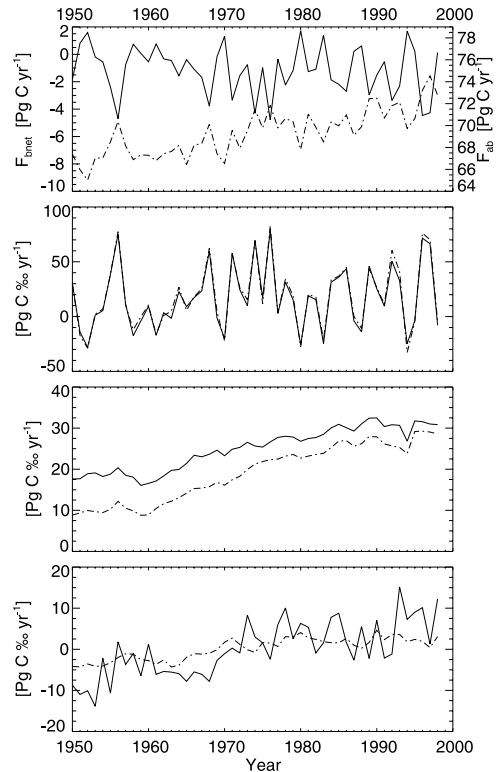

Figure 3. Global annual time-series of modelled F_{bnet} (solid line, negative values indicate net storage in land biosphere) and F_{ab} (dashed line), top panel, and the three terms giving the time dependency of $\delta^{13}C_a$ (see equation 4; in the following: solid ISOVAR and dashed ISOFIX): upper middle panel influence of the net flux (first term), lower middle panel Suess-Effect (second term) and bottom panel $\Delta^{13}F_{ab}$ (third term).

experiment is mainly a climate effect and most likely a response of the plants to increased water stress due to global warming during the 20th century. For the same time period, *McGuire et al.* [2001] already found a small declining trend in NPP leading to net carbon loss when considering climate only.

[14] Globally averaged time-series of the three terms yielding the temporal variations in atmospheric $\delta^{13}C_a$ from equation 4 and their corresponding CO_2 fluxes (F_{ab} and F_{bnet}, top panel) are plotted in Figure 3. The net atmosphere-biosphere flux (F_{bnet}) shows mainly an uptake of carbon by the land biosphere for the last 50 years, the amount of uptake is comparable to other model studies [*McGuire et al.*, 2001]. Interannual variability in the net flux is related to the variability in the El Niño Southern Oscillation (ENSO) [*Keeling et al.*, 1989]. As F_{bnet} is the same for both experiments, the values from the first term representing the influence of the net flux (upper middle panel) are almost identical for both experiments.

[15] A secular increasing trend in the terrestrial Suess-Effect from 17.5 PgC ‰ yr^{-1} in 1950 to more than 30 PgC ‰ yr^{-1} in 1998 caused by the invasion of isotopically light anthropogenic CO_2 into the biosphere is simulated (lower middle panel in Figure 3). High frequency (interannual) variability is strongly reduced as the ^{13}C entering the terrestrial biosphere is damped in the $\delta^{13}C_b$ emitted from

Figure 2. Global annual time-series of modelled discrimination against ^{13}C during photosynthesis, solid line ISOVAR and dashed line ISOFIX.

the biosphere because of the relatively long residence time of carbon in the land biosphere. The offset between the two experiments is caused by the difference in the fractionation factor at the beginning of the simulation period as mentioned above.

[16] The bottom panel of Figure 3 displays $\Delta^{13}F_{ab}$. Calculating $\Delta^{13}F_{ab}$ using the mean global average $\overline{\epsilon_{ab}}$ for the years 1920–1995 gives the magnitude of changes in the $^{13}CO_2$ fluxes due to climate variability in the fractionation factor ϵ_{ab} opposed to a constant ϵ_{ab}. In Table 1 the differences in the interannual variability of $\Delta^{13}F_{ab}$ are summarized. In the ISOFIX experiment the variations are only about 4 PgC ‰ yr^{-1}, whereas the ISOVAR experiment with climatic dependent discrimination exhibits interannual variations up to 15 PgC ‰ yr^{-1}. The difference in the variability in $\Delta^{13}F_{ab}$ between the two experiments is controlled only by the impact of climate variability on isotope discrimination during photosynthesis. In general, interannual variability is especially pronounced during pronounced ENSO events (e.g., 1992/93 and 1997/98) which lead through widespread drought conditions to a decrease in the isotopic fractionation factor.

[17] Using a variable climatic dependent discrimination in double deconvolution studies would certainly lead to a modification of the derived terrestrial sinks. Taking a variable fractionation factor into account we estimate that this could lead to a year-to-year shift of up to 0.8 PgC yr^{-1} in the inferred partitioning between terrestrial and oceanic carbon sinks. In general, a transient decrease in the terrestrial isotopic discrimination factor would imply a corresponding reduction in the inferred terrestrial source by means of a double deconvolution calculation.

4. Conclusions

[18] This study demonstrates that large interannual variations in ^{13}C fractionation, induced by anomalous climate events (e.g., ENSO) have a strong impact on the globally integrated terrestrial $^{13}CO_2$ fluxes. These fluctuations result primarily from plant physiological responses and to a minor extent from changes in vegetation composition (shifts between C_3- and C_4-plants) induced by climate variations. Ignoring these effects in global double deconvolution studies may result in significant errors in the inferred annual net atmosphere-biosphere flux of up to 0.8 PgC/yr, more than half of the global estimated biospheric sink during the 1990's [*Francey et al.*, 1995]. So far, these simulations do not consider land use change which influences the global discrimination values mainly through tropical C_4-pastures [*Townsend et al.*, 2002] and C_4-crops, e.g., maize cultivation in the northern hemisphere. However, we assume that the effect of land use change on the interannual variability is small compared to the climate effect. Future inverse modeling studies, which may lead to important revision of published carbon budgets for the past two decades, may wish to use the isotope LPJ framework for prescribing variations in terrestrial isotopic discrimination.

References

Ciais, P., P. P. Tans, M. Trolier, J. W. C. White, and R. J. Francey, A large northern hemisphere terrestrial CO_2 sink indicated by the $^{13}C/^{12}C$ ratio of atmospheric CO_2, *Science*, *269*, 1995.

Ekblad, A., and P. Högberg, Natural abundance of ^{13}C in CO_2 respired from forest soils reveals speed of link between tree photosynthesis and root respiration, *Oecologia*, *127*, 305–308, 2001.

Francey, R. J., P. P. Tans, C. E. Allison, I. G. Enting, J. W. C. White, and M. Trolier, Changes in oceanic and terrestrial carbon uptake since 1982, *Nature*, *373*, 326–330, 1995.

Francey, R. J., C. E. Allison, D. M. Etheridge, C. M. Trudinger, I. G. Enting, M. Leuenberger, R. L. Langenfelds, E. Michel, and L. P. Steele, A 1000-year high precision record of $\delta^{13}C$ in atmospheric CO_2, *Tellus*, *51B*, 170–193, 1999.

Fung, I., et al., Carbon 13 exchanges between the atmosphere and biosphere, *Glob. Biogeochem. Cycles*, 11, 1997.

Heimann, M., and E. Maier-Reimer, On the relations between the oceanic uptake of CO_2 and its carbon isotopes, *Glob. Biogeochem. Cycles*, *10*, 89–110, 1996.

Joos, F., and M. Bruno, Long-trem variability of the terrestrial and oceanic carbon sinks and the budgets of the carbon isotopes ^{13}C and ^{14}C, *Glob. Biogeochem. Cycles*, *12*, 277–295, 1998.

Kaplan, J. O., I. C. Prentice, and N. Buchmann, The stable carbon isotope composition of the terrestrial biosphere: Modeling at scales from leaf to the globe, *Global Biogeochem. Cycles*, *16*(4), 1060, doi:10.1029/2001GB001403, 2002.

Keeling, C. D., R. B. Bacastow, A. F. Carter, S. C. Piper, T. P. Whorf, M. Heimann, W. G. Mook, and H. Roeloffzen, A three-dimensional model of the atmospheric CO_2 transport based on observed winds: 1, Analysis of observational data, in *Aspects of Climate Variability in the Pacific and the Western Americas*, edited by D. H. Peterson, vol. 55, pp. 165–236, AGU, Washington, D.C., 1989.

Lloyd, J., and G. Farquhar, ^{13}C discrimination during CO_2 assimilation by the terrestrial biosphere, *Oecologia*, *99*, 201–215, 1994.

Marland, G., T. A. Boden, and R. J. Andres, Global, regional, and national CO_2 emissions, in *Trends: A Compendium of Data on Global Change*, Carbon Dioxide Information Analysis Center, Oak Ridge National Laboratory, U.S. Department of Energy, Oak Ridge, Tenn., U.S.A., 2001.

McGuire, A. D., et al., Carbon balance of the terrestrial biosphere in the twentieth century: Analyses of CO_2, climate and land use effects with four process-based ecosystem models, *Glob. Biogeochem. Cycles*, *15*, 183–206, 2001.

Mook, W. G., ^{13}C in atmospheric CO_2, *Neth. J. Sea Res.*, *20*, 211–223, 1986.

New, M., M. Hulme, and P. Jones, Representing twentieth-century space-time climate variability, Part II: Development of 1901–96 monthly grids of terrestrial surface climate, *Climate. J.*, *13*, 2217–2238, 2000.

Prentice, I. C., The carbon cycle and atmospheric carbon dioxide, in *Climate Change 2001: The Scientific basis*, edited by J. T. Houghton, Y. Ding, D. J. Griggs, M. Noguer, P. J. van der Linden, X. Dai, K. Maskell, and C. A. Johnson, pp. 183–237, Cambridge University Press, Cambridge, 2001.

Sitch, S., I. C. Prentice, and B. Smith, LPJ – a coupled model of vegetation dynamics and the terrestrial carbon cycle, in *The role of vegetation dynamics in the control of atmospheric CO_2 content*, S. Sitch, Ph.D. thesis, Lund University, Lund, 2000.

Tans, P. P., J. A. Berry, and R. F. Keeling, Oceanic $^{13}C/^{12}C$ observations: A new window on ocean CO_2 uptake, *Glob. Biogeochem. Cycles*, *7*, 353–368, 1993.

Townsend, A. R., G. P. Asner, J. W. C. White, and P. P. Tans, Land use effects on atmospheric ^{13}C imply a sizable terrestrial CO_2 sink in tropical latitudes, *Geophys. Res. Let.*, *29*, 68-1–68-4, 2002.

———————
M. Scholze, Max-Planck-Institut für Meteorologie, Bundesstr. 55, 20146 Hamburg, Germany. (scholze@dkrz.de)

W. Knorr, M. Heimann, Max-Planck-Institut für Biogeochemie, Carl-Zeiss-Promenade 10, 07745 Jena, Germany.

J. O. Kaplan, Canadian Centre for Climate Modeling and Analysis, P.O. Box 1700, STN CSC, Victoria, B.C., V8W 2Y2, Canada.